

Comprehensive Two-Dimensional Gas Chromatography Coupled to Time of Flight Mass Spectrometry: New Biomarker Parameter Proposition for the Characterization of Biodegraded Oil

Renata F. Soares,*^a Ricardo Pereira,^a Raphael S. F. Silva,^a Leonardo Mogollon^b and Débora A. Azevedo*^a

^aInstituto de Química, Universidade Federal do Rio de Janeiro, Ilha do Fundão, 21941-909 Rio de Janeiro-RJ, Brazil

^bInstituto Colombiano del Petroleo, ECOPEL S. A., Bucaramanga, Colombia

Cromatografia gasosa bidimensional abrangente acoplada à espectrometria de massas por tempo de voo (GC×GC-TOFMS) é uma técnica apropriada para a elucidação da composição molecular de amostras petroquímicas, como óleos biodegradados. Biomarcadores foram separados, identificados e razões de biomarcadores convencionais foram determinados usando cromatografia gasosa acoplada à espectrometria de massas (GC-MS) e GC×GC-TOFMS. No cromatograma de íons extraídos m/z 123 + 177 + 191, coeluições entre terpanos tricíclicos, hopanos e 25-*nor*-hopanos com secohopanos foram resolvidas usando GC×GC-TOFMS. GC×GC-TOFMS permitiu a identificação da série completa dos 25-*nor*-hopanos, *nor*-gammacerano, C₂₉ 28-*nor*-espergulano e oleanano, que não foram identificados por GC-MS. A avaliação dos parâmetros geoquímicos dos óleos estudados indicou uma origem marinha e um ambiente deposicional sob condições anóxicas. A alta resolução cromatográfica e sensibilidade alcançada usando GC×GC-TOFMS permitiram sugerir três novos parâmetros geoquímicos para a caracterização de óleos altamente biodegradados. Estes resultados demonstram a superioridade da técnica GC×GC-TOFMS na separação e identificação de compostos individuais e não-alvos em óleos severamente biodegradados.

Comprehensive two-dimensional gas chromatography with time of flight mass spectrometry (GC×GC-TOFMS) is an appropriate technique for the elucidation of molecular composition of petrochemical samples, such as biodegraded oils. Biomarkers were separated and identified, and conventional biomarker ratios were determined via gas chromatography-mass spectrometry (GC-MS) and GC×GC-TOFMS. In the extracted ion chromatogram m/z 123 + 177 + 191, coelutions between tricyclic terpanes, hopanes and 25-*nor*-hopanes with secohopanes were resolved by GC×GC-TOFMS. GC×GC-TOFMS allowed the identification of complete series of 25-*nor*-hopanes, *nor*-gammacerane, C₂₉ 28-*nor*-spergulanes and oleanane not identified by using GC-MS. The biomarker ratios from the studied oils indicated that they derived from marine source rock deposited under anoxic conditions. The higher chromatographic resolution and sensitivity achieved by using GC×GC-TOFMS allowed for three new parameters to characterize biodegraded oils. These results indicated the superiority of GC×GC-TOFMS for separation and identification of individual and non-target compounds in severely biodegraded oils.

Keywords: heavily biodegraded oils, biomarker, geochemical parameters, comprehensive two-dimensional gas chromatography, time of flight mass spectrometry

Introduction

Crude oil in subsurface petroleum reservoirs can undergo alteration processes, which results in aerobic and/or anaerobic

degradation promoted by microorganisms.^{1,2} The final result of this biological activity in the deep subsurface is the biodegradation of oils. The effects of biodegradation on the composition of crude oil are relatively well-known. Scales of chemical changes occurring during the biodegradation are provided in various publications,³⁻⁵ with the Peters and

*e-mail: renata_filgueiras@yahoo.com.br, debora@iq.ufrj.br

Moldowan (PM) biodegradation scale most commonly used.⁵ The general removal sequence of saturated hydrocarbon compound classes during biodegradation includes the following: *n*-alkanes, alkylcyclohexanes, acyclic isoprenoid alkanes, bicyclic alkanes, steranes and hopanes. The generation of other hydrocarbons, such as secohopanes and 25-*nor*-hopanes, occurs when advanced levels of degradation are achieved.⁶ Biodegraded oils represent a significant fraction of the petroleum in conventional oil reserves, making their molecular composition complex. All biodegraded oils are also mixtures,⁷ making them even more complicated. This aspect leads to difficulties in evaluating the molecular composition of biodegraded oil samples.

Gas chromatography-mass spectrometry in tandem (GC-MS/MS) and conventional GC-MS are the chromatographic techniques most commonly used for the chemical and geochemical characterization of the petroleum samples.^{6,8,9} The main problem in GC-MS analyses is the coelution, which hampers the correct identification of many compounds, particularly in complex mixtures such as biodegraded oils. This can be solved by using GC-MS/MS through monitoring selective reaction. Full mass spectra of compounds, however, are not obtained with this technique. Mass spectra are particularly interesting when the focus of analysis is not only the search for known compounds but also for the search for new or non-target compounds that can provide new insights into the petroleum system under investigation. Comprehensive two-dimensional gas chromatography with time of flight mass spectrometry (GC×GC-TOFMS) is an option for overcoming the limitations of one-dimensional GC-MS (coelution) and GC-MS/MS (lack of full mass spectra). Thus, GC×GC-TOFMS is an appropriate technique for the elucidation of molecular composition of complex petrochemical samples, such as biodegraded oils. Recently, GC-MS, gas chromatography-mass spectrometry in *tandem* with multiple reaction monitoring (GC-MRM-MS) and GC×GC-TOFMS techniques were compared for the biomarker characterization in tertiary oils and rock extracts. In this work,⁹ the authors emphasize the outstanding capabilities of GC×GC-TOFMS for the separation of compounds with identical molecular masses and similar MS fragmentation.

The importance of GC×GC-TOFMS is demonstrated in several works in a variety of matrices, e.g., characterization of petrochemical samples and derivatives,¹⁰ biodegradation in petroleum¹¹ and mixtures diesel/biodiesel,¹² analysis of Fischer-Tropsch synthesis products¹³ and unresolved complex mixtures of hydrocarbons extracted from late Archean sediments,¹⁴ characterization of biomarker in Brazilian oils,¹⁵ in extra heavy gas oil (EHGO),¹⁶ and the study of unresolved complex mixtures (UCM) in the

maltene fractions of hydrothermal petroleum.¹⁷

There has only been one report published showing the use of GC×GC-TOFMS applied to biomarker analysis of oils from Colombia,¹⁸ in which conventional geochemical parameters based on biomarker ratios were used to analyze the source and maturity evaluation. Ventura *et al.*¹⁹ was the first study that used GC×GC-TOFMS in obtaining geochemical parameters. Before that, GC×GC-TOFMS was only used for qualitative biomarker analyses.

Many oils from the Colombian Basin are considered heavily biodegraded based on biomarker composition. As already presented, a full biomarker characterization of these oils is hard to obtain only via GC-MS and GC-MS/MS. Thus, the aim of our work is to show the usage of GC×GC-TOFMS for the analysis of biomarkers in heavily biodegraded oils from Colombia and the determination of conventional biomarker ratios based on GC-MS and GC×GC-TOFMS results. Last but not least, based on the same experiments, new biodegradation biomarker parameters are proposed.

Experimental

Samples and sample preparation

Four crude oil samples from Colombia were submitted to liquid chromatography. The samples were supplied by Ecopetrol (Bucaramanga, Colombia), and named Oils #1, #2, #3 and #4. The crude oil samples (ca. 100 mg) were dissolved in 0.5 mL of hexane and applied to the top of a mini-column (150 × 10 mm) containing 2.5 g of activated silica gel (120 °C overnight) and further rinsed with more 0.5 mL of the hexane and transferred to the column and this procedure was repeated 3 times. Then, samples were fractionated into saturated and aromatic hydrocarbons and polar compounds using *n*-hexane (8 mL), *n*-hexane:dichloromethane (8:2, v:v, 10 mL) and dichloromethane:methanol (9:1, v:v, 10 mL), respectively. The solvent from each fraction was evaporated and 500 µL of dichloromethane added. Saturated hydrocarbon fractions (1 µL) were analyzed by using GC-MS and GC×GC-TOFMS. Further details were previously reported.²⁰⁻²² The percentage of saturated hydrocarbons, aromatic hydrocarbons and polar compounds (SAP results), as calculated from the quantity weigh-out of the respective fractions, are presented in Table 1.

Chromatographic conditions

GC-FID

GC-FID analyses were performed with Agilent Technologies 7890N (Palo Alto, CA, USA), a gas

Table 1. SAP results. Chemical group-type composition for the samples

Compound	Oil #1	Oil #2	Oil #3	Oil #4
Saturated / %	23	40	48	54
Aromatic / %	15	30	28	31
Polar / %	39	9	13	10
Recovery / %	77	79	89	95

chromatograph coupled to a flame ionization detector. Separation was achieved with a HP5 fused silica column (30 m × 0.25 mm i.d., 0.25 μm film thickness). The GC oven operating conditions were 40 to 320 °C (10 min) at 6 °C min⁻¹. H₂ was used as carrier gas. Samples were injected in splitless mode with the injector temperature at 290 °C and detector temperature at 340 °C. The crude oil samples (10 mg) were dissolved in 500 μL of dichloromethane and analyzed by GC-FID.

GC-MS

GC-MS analyses were performed with an Agilent Technologies 6890N (Palo Alto, CA, USA) gas chromatograph coupled with the Agilent Technologies 5973 mass spectrometer. Separation was achieved with a HP5 fused silica column (30 m × 0.25 mm i.d., 0.25 μm film thickness). The GC oven operating conditions were 70 (1 min) to 170 °C at 20 °C min⁻¹ and 170 to 325 °C at 2 °C min⁻¹. He was used as carrier gas at a flow of 1.0 mL min⁻¹. Samples were analyzed in single ion monitoring and scan mode. Samples were injected in splitless mode with the injector temperature at 290 °C. GC-MS was operated in the 70 eV electron ionization (EI) mode with a collected mass range of 50-600 Da.

GC×GC-TOFMS and data processing

GC×GC-TOFMS analyses were performed with a Pegasus 4D system (Leco, St. Joseph, MI, USA) which consists of an Agilent Technologies 6890 gas chromatograph (Palo Alto, CA, USA) equipped with a secondary oven, a non-moving quad-jet dual-stage modulator and a Pegasus III mass spectrometer (Leco, St. Joseph, MI, USA). The data acquisition and processing method were carried out by using ChromaTOF™ software version 4.21 (Leco, St. Joseph, MI, USA). The GC column set consisted of a HP5 (5%-phenyl-95%-methylsiloxane; Agilent Technologies, Palo Alto, CA, USA) column (30 m, 0.25 mm i.d., 0.25 μm film thickness) as the first dimension (1D) and a BPX50 (50%-phenyl-50%-methylsiloxane; SEG, Ringwood, VIC, Australia) column (1.5 m, 0.1 mm i.d., 0.1 μm film thickness) as the second dimension (2D). The second

column was connected to the TOFMS instrument (Leco, St. Joseph, MI, USA) via an uncounted deactivated silica tube (0.5 m × 0.25 mm i.d.). The columns and the empty deactivated column were connected by SilTite™ mini-unions and metal ferrules made for 0.10-0.25 mm i.d. GC columns (SEG, Ringwood, VIC, Australia).

The temperature program used in the first column (1D) was: 70 (1 min) to 170 °C at 20 °C min⁻¹ and 170 to 325 °C at 2 °C min⁻¹. The programming for the second column consisted of a gradient of 10 °C above the first column: 80 (1 min) to 180 °C at 20 °C min⁻¹ and 180 to 335 °C at 2 °C min⁻¹. The modulator temperature was 30 °C above the temperature of the first column and the modulation period was 8 s, with a 2 s cold jet and a 2 s hot jet. He was used as carrier gas at a flow of 1.5 mL min⁻¹. The temperatures of the transfer line to the mass spectrometer and the ion source were 280 and 230 °C, respectively. The detector was operated at 1650 V and the acquisition rate was 100 spectra s⁻¹. Samples were injected in splitless mode with the injector temperature at 290 °C. TOFMS was operated in the electron impact ionization mode at 70 eV. The analyzed mass range was 50-600 Da.

Samples were evaluated from total ion chromatograms (TIC) and extracted ion chromatograms (EIC) by using *m/z* 85 (paraffins), *m/z* 191 (tri-, tetra- and pentacyclic terpanes, gammacerane, oleanane), *m/z* 177 (C₁₀ demethylated tri-, tetracyclic terpanes and 17α(H)-25-nor-hopanes), *m/z* 341 (25,28-nor-hopanes), *m/z* 369 (28-nor-spergulananes), *m/z* 217 and 218 (ααα and αββ steranes, respectively), *m/z* 123 (secohopanes) and *m/z* 259 (diasteranes and tetracyclic polyprenoids) as diagnostic ions, based on previous works.^{16,23}

After data acquisition and processing by the use of ChromaTOF™ software version 4.21, individual peak areas were automatically acquired and individual compound identification was performed by the comparison with the literature and standard compound mass spectra by examination, interpretation of MS fragmentation patterns, retention time, and elution order of compounds.²⁴⁻²⁸

Results and Discussion

Initially, the heavily biodegraded whole oil samples from Colombia were analyzed using GC-FID to provide a rapid assessment of oil composition. Then, the saturated hydrocarbon fractions, after fractioning, were analyzed by GC-MS and GC×GC-TOFMS. The whole oil (GC-FID) chromatogram from the oil samples and the GC-MS mass chromatograms from the saturated hydrocarbon fractions are shown in Figure S1 (in the Supplementary Information (SI) section).

Chromatographic aspects

The comparison between GC-MS and GC×GC-TOFMS was performed in order to emphasize the increase in the chromatographic resolution and sensitivity achieved using GC×GC-TOFMS. Because of the complexity of the biodegraded oil samples, no additional chemical information could be obtained from GC-MS due to the large number of components and limited separation capacity. The acquired GC-MS data revealed coelutions that involved important compound classes such as secohopanes, hopanes and demethylated hopanes, as shown in Figure 1, curves a-c. In the two-dimensional chromatogram (Figure 1d), several of these coelutions were resolved, such as 25,28,30-tris-*nor*-hopane (25,28,30-TNH) from C₃₀ 8,14-secohopane (SH30), and C₃₀ 17 α (H),21 β (H)-30-hopane (H30) from 17 α (H),21 β (H)-25-*nor*-30-hopane (D30R), and C₃₁ 8,14-secohopane (SH31), as shown in Figure 2. The separation between H30 and D30R has previously been reported,¹⁶ but in the present work, it was also observed the separation of another compound in this region, the C₃₁ 8,14-secohopane (SH31). In addition, the structured chromatogram allowed a better identification of compounds by classes in the chromatographic plane, especially the secohopanes, present in low concentrations.

The *nor*-spergulane and *nor*-gammacerane were not detected by GC-MS because of either low concentration or occurrence of possible coelutions. The C₂₉ 28-*nor*-spergulane (29NSP), the main member of the previously identified series as 28-*nor*-spergulanes,²⁷ was detected and recognized using GC×GC-TOFMS, as shown in Figure 3. This compound is a rearranged hopane and exhibits a mass spectrum typical of hopanes, with a base peak at *m/z* 191. However, the fragment *m/z* 369 is more intense in this compound than in regular hopanes (Figure S4, in the SI section). The compound eluted between the C₂₉ and C₃₀ hopanes (Figure 3). The geochemical implications of 28-*nor*-spergulanes are not well-known, even though they are detected in a large number of oils from different sources. 28-*nor*-spergulane is particularly abundant in lacustrine oils from Southeast Asia. This biomarker has also been detected in Brazilian¹⁶ and Colombian oils¹⁸ by GC×GC-TOFMS. Another series of rearranged hopanes known as 18 α -neohopanes (Ts, C₂₉Ts) were also identified, along with their demethylated products.

Nytoft *et al.*²⁷ detected a pentacyclic terpane, the last C₂₉ terpane in the chromatographic run, which eluted after H30. By examining the mass spectrum in that work,²⁷ this compound was tentatively identified by the authors as 24-*nor*-gammacerane. But this was, however, based on a synthetic compound and not on a natural one. In the

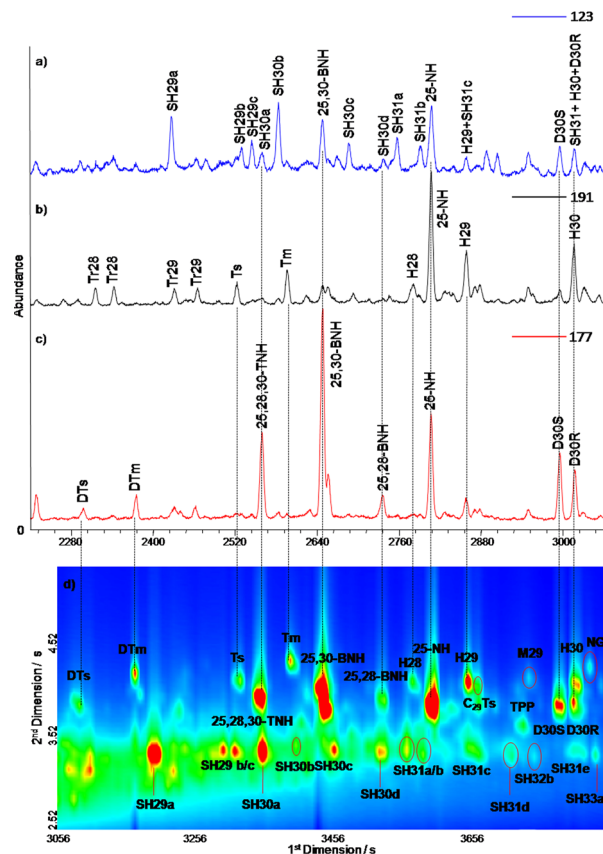


Figure 1. Saturated hydrocarbon fraction from Oil #2: (a) GC-MS *m/z* 123 mass chromatogram; (b) *m/z* 191 mass chromatogram; (c) *m/z* 177 mass chromatogram and (d) GC×GC-TOFMS overlaid EIC *m/z* 191, 177 and 123 of the same sample, showing the separation and identification of biomarkers and solved coelutions in 2D. Note the separation achieved for hopanes, 25-*nor*-hopanes and secohopanes in 2D. DTs: 18 α (H),21 β (H)-22,25,29,30-tetranorhopane; DTm: 17 α (H),21 β (H)-22,25,29,30-tetra-*nor*-hopane; Ts: 18 α (H),21 β (H)-22,29,30-trisnorhopane; Tm: 17 α (H),21 β (H)-22,29,30-tris-*nor*-hopane; 25,28,30-TNH: 17 α (H),18 α (H),21 β (H)-25,28,30-tris-*nor*-hopane; 25,30-BNH: 17 α (H),18 α (H),21 β (H)-25,30-bis-*nor*-hopane; 25,28-BNH: 17 α (H),18 α (H),21 β (H)-25,28-bis-*nor*-hopane; H28: 17 α (H),18 α (H),21 β (H)-28,30-bis-*nor*-hopane; 25-NH: 17 α (H),21 β (H)-25-*nor*-hopane; H29: 17 α (H),21 β (H)-30-*nor*-hopane; C29Ts: 18 α (H),21 β (H)-30-*nor*-neohopane; TPP: Tetracyclic polyprenoid; M29: 17 β (H),21 α (H)-30-*nor*-hopane; H30: C₃₀ 17 α (H),21 β (H)-hopane; Hn: C_n hopane; D30: demethylated C₃₁ hopane NG: *nor*-gammacerane; SH: secohopane. To more abbreviation identification see also Table S1 (in the SI section).

present work, a compound was also found eluting after H30 on the second column. It is possible that this compound is 25-*nor*-gammacerane (Figure 4) as all detected demethylated hopanoids and tricyclic terpenoids are usually 25-*nor*. Why would biodegradation act on C24- and not on the well-known C25-position? For this reason, this compound was tentatively identified as either 25-*nor*-gammacerane, or only as *nor*-gammacerane, as not known for sure the exact demethylation position. This reinforces the hypothesis that it may be a *nor*-gammacerane because its precursor (gammacerane) also interacted more with the 2D column

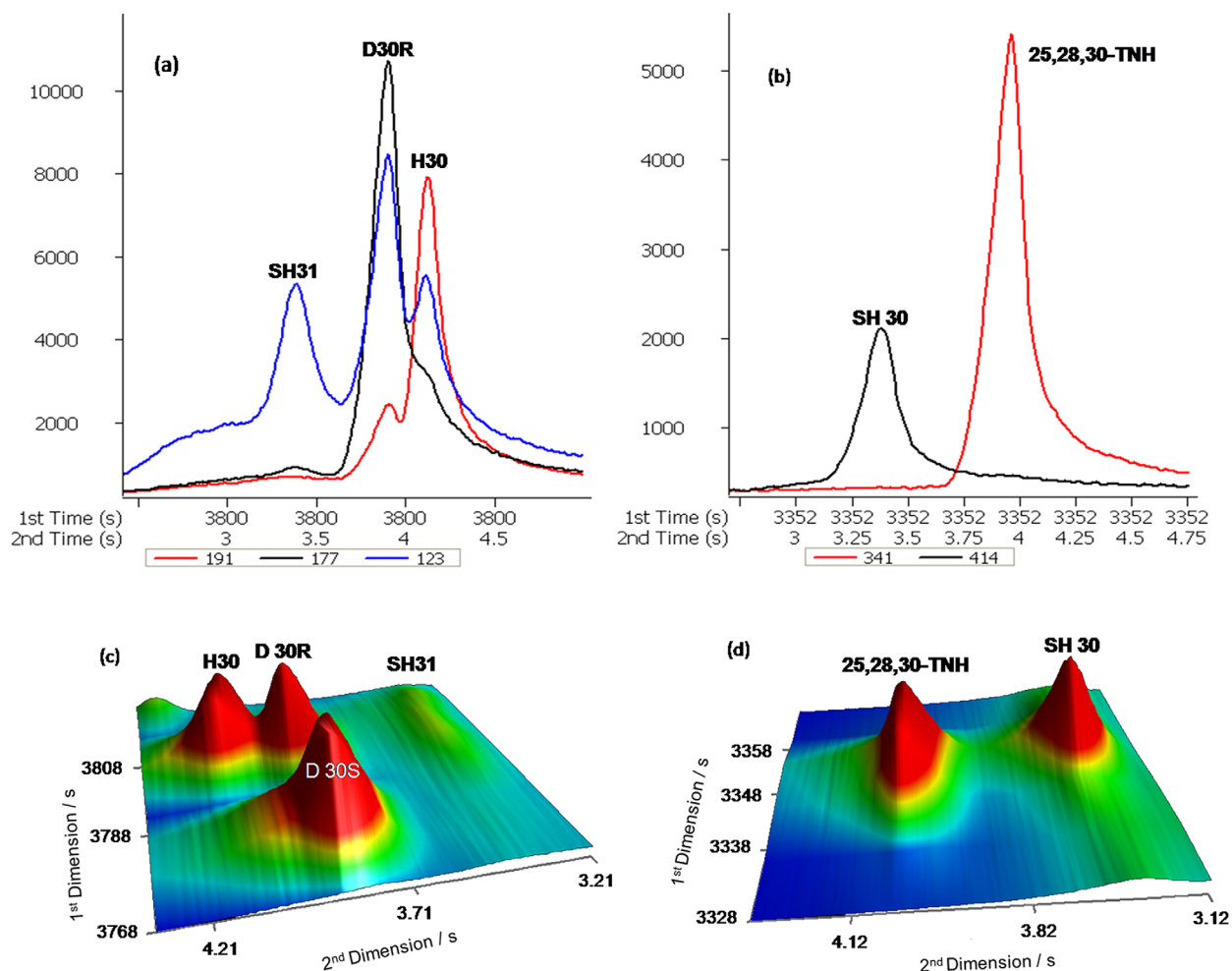


Figure 2. GCxGC-TOFMS m/z 191, 177 and 123 EIC of saturated hydrocarbon fraction from Oil #2, showing the separation and identification of biomarkers and solved coelution problems: (a) and (b) expansion chromatograms in the first dimension; (c) and (d) tri-dimensional chromatograms.

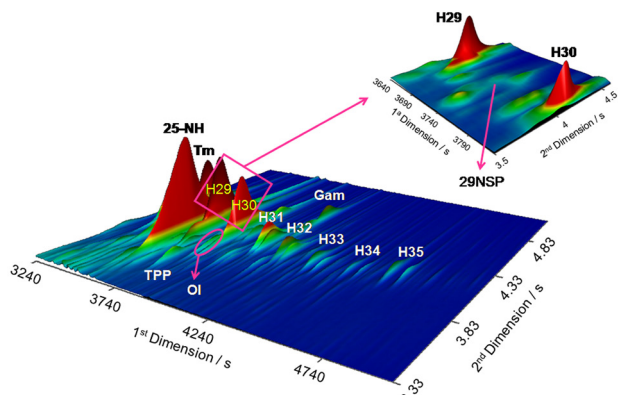


Figure 3. GCxGC-TOFMS EIC m/z 191 of saturated hydrocarbon fraction from Oil #2, showing the identification of hopanes, with details for 28-*nor*-spergulane and oleanane at low abundances. 25-NH: 17 α (H),21 β (H)-25-*nor*-hopane; Tm: 17 α (H),21 β (H)-22,29,30-trisnorhopane; H29: 17 α (H),21 β (H)-30-*nor*-hopane; TPP: tetracyclic polyprenoid; H30: C₃₀ 17 α (H),21 β (H)-hopane; Hn: C_n hopane; Gam: gammacerane; OI: oleanane; 29NSP: C₂₉ 28-*nor*-spergulane. To abbreviation identifications see also Table S1 (in the SI section).

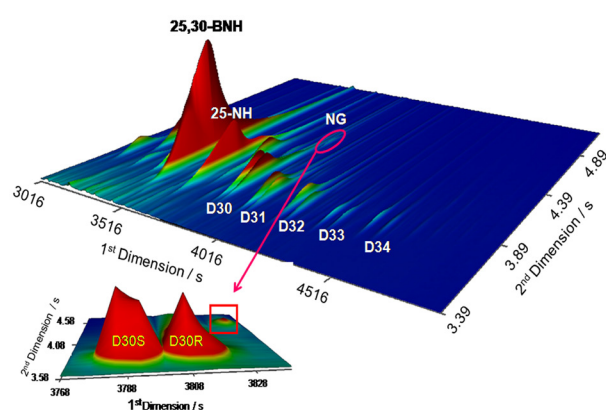


Figure 4. GCxGC-TOFMS EIC m/z 177 of saturated hydrocarbon fraction from Oil #2, showing the identification of demethylated hopanes (25-*nor*-hopanes), with details for *nor*-gammacerane identification. 25,30-BNH: 17 α (H),18 α (H),21 β (H)-25,30-bis-*nor*-hopane; 25-NH: 17 α (H),21 β (H)-25-*nor*-hopane; NG: *nor*-gammacerane; D30: demethylated C₃₁ hopane, Dn: demethylated C_{n+1} hopane. To abbreviation identifications see also Table S1 (in the SI section).

due to differences in chemical structure: gammacerane is a hexacyclic terpenoid while hopane is a pentacyclic terpenoid. Thus, the separation in the second dimension allowed one to distinguish between hopane and gammacerane families in the chromatographic plane (Figure 5).

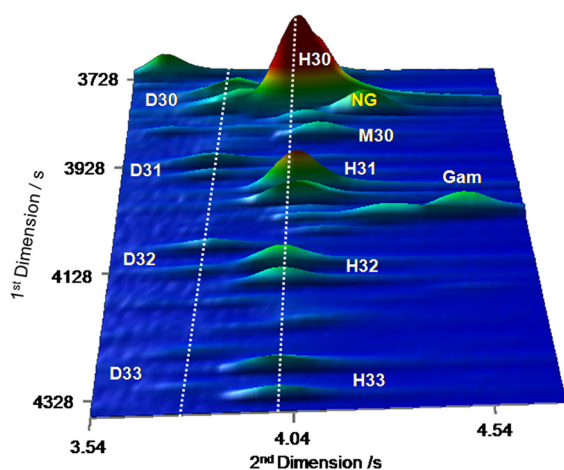


Figure 5. GCxGC-TOFMS EIC m/z 191 and 177 of saturated hydrocarbon fraction from Oil #2, showing the distinction between the homohopane and gammacerane families. H30: C_{30} $17\alpha(H),21\beta(H)$ -hopane; Hn: Cn hopane; Gam: gammacerane NG: *nor*-gammacerane; D30: demethylated C_{31} hopane, Dn: demethylated C_{n+1} hopane. To more abbreviation identifications see also Table S1 (in the SI section).

Geochemical interpretation

Geochemical parameters are used to provide maximum geological interpretations to help solving problems in the production, development, exploration, environmental and archaeological problems. Thus, geochemical correlations using biomarkers provide a better understanding of the relationship of the reservoir, thereby improve the exploration success by establishing possible routes of oil migration. For this reason, the identification of biomarkers is widely used in oil-oil correlation and oil-source rock, being a powerful tool in oil exploration. Furthermore, the use of biomarker ratios provides important information concerning the origin, thermal maturation and biodegradation of oils. The characterization of depositional environments of petroleum source rocks using biomarker parameters provides criteria for distinguishing source rocks deposited in different environments, such as lacustrine and marine. The thermal maturity term refers to the thermal reactions resulting from the progress of increase in temperature that leads to the conversion of organic material in sedimentary oil. The biodegradation of the oil consists of a series of biological processes that cause preferential removal of some compounds attacked by microorganisms, altering the composition of petroleum. The quality of the oil and its liquid volume decreases with an increase in biodegradation.

Thus, it can significantly impact the economic value and production of oil.

The geochemical parameters calculated for the samples using GC-MS and GCxGC-TOFMS are given in Table 2.

Depositional environment

Parameters such as Hop/St (1, Table 2), H30/C27 $\alpha\alpha\alpha$ (2), percentage of steranes (3), Ts/Tm (4), Te24/H30 (9) and H35/H34 (11) were obtained in order to evaluate the depositional environment. The hopane/steranes (Hop/St) ratio obtained from Oils #2, #3 and #4 ranged from 0.9 to 1.08 as measured by GCxGC-TOFMS, and between 1.08 to 1.46 as measured by GC-MS (Table 2). This indicates marine organic matter deposition revealed by both techniques (Hop/St < 4.0). The finding is consistent with the predominance of C_{27} steranes over homologue C_{29} and with the presence of C_{30} sterane. Low concentrations of Tr19 and Tr20 compared to Tr23 in all samples are also indicative of marine oils.^{6,29} The Ts/Tm ratios of the Oils #2, #3 and #4 using GC-MS and GCxGC-TOFMS were below 1, indicating a marine carbonate or evaporate depositional environment.²⁹

High H35/H34 ratios (> 1) revealed the selective preservation of the C_{35} homologue and indicate that the oils were derived from a marine source rock deposited under low redox conditions.⁵ High concentrations of C_{35} homohopane in Oils #2, #3 and #4 using both GC-MS and GCxGC-TOFMS are indicative of anoxic conditions during source-rock deposition.⁶ The presence of 25,28,30-TNH in all samples indicates that the oil samples are most likely derived from anoxic marine depositional environment oils.⁶

The C_{24} tetracyclic terpane/hopane ratio (Te24/H30) increases in more mature source rocks and oils as a result of the greater stability of the tetracyclic terpanes. They also appear more resistant to biodegradation than hopanes⁶. For these reasons, they can be used in correlations of altered petroleum. The presence of C_{24} tetracyclic terpanes for all of the oil samples are thought to be common in carbonate and evaporite depositional environments.^{29,30}

Other pentacyclic terpanes, such as gammacerane and oleanane, were also identified using GCxGC-TOFMS (Figure 3) but not detected via GC-MS. These compounds are highly resistant to biodegradation.²⁶ However, Oils #2, #3 and #4 showed Gam/H30 ratios higher than 0.11, indicating salinity and water column stratification in the source rock depositional environment. This was also used as an indicator of carbonate and evaporitic environments.²⁹ In addition, high Ol/H30 ratio is indicative of terrestrial environments.⁶ Low Ol/H30 ratios were found for Oils #2 and #4, suggesting marine depositional environments.

Maturity

Parameters such as H32 $S/(S + R)$ (12, Table 2), $Ts/(Ts + Tm)$ (13), $C_{29} \alpha\alpha\alpha S/(S + R)$ (14) and $C_{29} \beta\beta/(\alpha\alpha + \beta\beta)$ (15) steranes were obtained in order to evaluate the thermal maturity.

The H32 $S/(S + R)$ ratio increases from zero to approximately 0.6, with equilibrium values in the range from 0.57 to 0.62 during thermal maturation.^{6,31} Samples whose ratios are between 0.50 to 0.54 barely entered the oil generation range, as observed for the Oils #2 and #4 by using GC-MS and Oil #3, both via GC-MS and

Table 2. Geochemical data showing selected source, thermal evolution and biodegradation parameters of samples via GC-MS and GC×GC-TOFMS

Parameter	Oil #1		Oil #2		Oil #3		Oil #4	
	GC-MS	GC×GC-TOFMS	GC-MS	GC×GC-TOFMS	GC-MS	GC×GC-TOFMS	GC-MS	GC×GC-TOFMS
Hop/St ¹	nd	nd	1.08	0.90	1.16	0.99	1.46	1.08
H30/C ₂₇ $\alpha\alpha\alpha$ ²	nd	nd	1.09	1.55	1.08	0.97	1.58	1.87
C ₂₇ ³ / %	nd	nd	37.4	49.0	40.3	41.8	38.6	42.6
C ₂₈ / %	nd	nd	36.4	34.4	29.7	27.7	33.0	33.7
C ₂₉ / %	nd	nd	26.2	16.6	30.0	30.5	28.4	23.6
Ts/Tm ⁴	nd	nd	0.63	0.57	0.60	0.70	0.65	0.64
Gam/H30 ⁵	nd	nd	nd	0.11	nd	0.33	nd	0.16
Ol/H30 ⁶	nd	nd	nd	0.08	nd	nd	nd	0.10
H29/H30 ⁷	nd	nd	0.80	0.79	0.90	1.00	0.88	0.64
Tr23/H30 ⁸	2.62	7.77	1.91	8.66	1.50	3.89	1.38	5.91
Te24/H30 ⁹	0.60	1.04	0.44	0.80	0.37	0.64	0.31	0.53
Tr25/Tr26 ¹⁰	1.57	0.89	0.57	0.74	0.58	1.05	0.62	1.74
H35/H34 ¹¹	nd	nd	1.39	1.39	1.29	1.49	1.31	1.57
H32 $S/(S + R)$ ¹²	nd	nd	0.51	0.56	0.53	0.54	0.54	0.57
Ts/(Ts + Tm) ¹³	nd	nd	0.39	0.36	0.37	0.41	0.40	0.39
C ₂₉ $\alpha\alpha\alpha S/(S + R)$ ¹⁴	nd	nd	0.51	0.53	0.60	0.43	0.58	0.67
C ₂₉ $\beta\beta/(\alpha\alpha + \beta\beta)$ ¹⁵	nd	nd	0.51	0.55	0.53	0.80	0.54	0.57
25-NH/H30 ¹⁶	3.45	6.04	1.58	2.38	1.33	2.14	1.11	1.36
25,28,30-TNH/H30 ¹⁷	2.01	2.54	1.59	2.05	1.23	1.49	0.95	0.99
New parameter								
25,30-BNH/H30 ¹⁸	5.79	12.53	4.06	6.12	3.29	4.87	2.66	3.83
25,28-BNH/H30 ¹⁹	1.27	1.02	0.44	0.47	0.44	0.45	1.11	0.35
SH30a/H30 ²⁰	2.77	13.56	1.13	7.58	0.97	5.99	0.68	2.23

nd: not detected; ¹Calculated from peak areas of Σ H29-H35 hopanes in the m/z 191 chromatogram over peak areas of Σ C₂₇-C₂₉ steranes in the m/z 217 chromatogram. Hop/St: (H29-H35)/[C₂₇, C₂₈, C₂₉ $\alpha\alpha\alpha$ (20S + 20R) and $\alpha\beta\beta$ (20S + 20R)] (m/z 191 and 217). ²Calculated from peak area of C₃₀ 17 α (H), 21 β (H)-30-hopane in the m/z 191 chromatogram over peak areas of C₂₇ 5 α (H), 14 α (H), 17 α (H)-cholestanes (20S + 20R) in the m/z 217 chromatogram. H30/C₂₇ $\alpha\alpha\alpha$: (H30)/C₂₇ $\alpha\alpha\alpha$ (20S + 20R). ³Calculated from % C₂₇ sterane (m/z 217): 100 [C₂₇ $\alpha\alpha\alpha$ (20S + 20R) + C₂₇ $\alpha\beta\beta$ (20S + 20R)] / [(C₂₇ $\alpha\alpha\alpha$ (20S + 20R) + C₂₇ $\alpha\beta\beta$ (20S + 20R) + C₂₈ $\alpha\alpha\alpha$ (20S + 20R) + C₂₈ $\alpha\beta\beta$ (20S + 20R) + C₂₉ $\alpha\alpha\alpha$ (20S + 20R) + C₂₉ $\alpha\beta\beta$ (20S + 20R)]. ⁴Calculated from peak area of 18 α (H), 21 β (H)-22,29,30-tris-*nor*-neohopane (Ts) over peak area of 17 α (H), 21 β (H)-22,29,30-tris-*nor*-hopane (Tm) in the m/z 191 chromatogram. ⁵Calculated from peak area of gammacerane (Gam) over peak area of C₃₀ 17 α (H), 21 β (H)-30-hopane (H30) in the m/z 191 chromatogram. ⁶Calculated from peak area of oleanane (Ol) over peak area of C₃₀ 17 α (H), 21 β (H)-30-hopane (H30) in the m/z 191 chromatogram. ⁷Calculated from peak area of 17 α (H), 21 β (H)-29-hopane (H29) over peak area of C₃₀ 17 α (H), 21 β (H)-30-hopane (H30) in the m/z 191 chromatogram. ⁸Calculated from peak area of C₂₃ tricyclic terpane (Tr23) over peak area of C₃₀ 17 α (H), 21 β (H)-30-hopane (H30) in the m/z 191 chromatogram. ⁹Calculated from peak area of C₂₄ tetracyclic terpane (Te24) over peak area of C₃₀ 17 α (H), 21 β (H)-30-hopane (H30) in the m/z 191 chromatogram. ¹⁰Calculated from peak area of C₂₅ tricyclic terpane (Tr25) over peak area of C₂₆ tricyclic terpanes (Tr26) in the m/z 191 chromatogram. ¹¹Calculated from peak area of 17 α (H), 21 β (H)-tetrakisohomohopane (22S + 22R) (H34) over peak areas of 17 α (H), 21 β (H)-pentakisohomohopane (22S + 22R) (H35) in the m/z 191 chromatogram. H34/H35: [H34 (22S + 22R) / H35 (22S + 22R)] (m/z 191). ¹²Calculated from peak areas of H32 17 α (H), 21 β (H)-bishomohopane (22S + 22R) in the m/z 191 chromatogram. ¹³Calculated from peak areas of 18 α (H), 21 β (H)-22,29,30-tris-*nor*-neohopane (Ts) and 17 α (H), 21 β (H)-22,29,30-tris-*nor*-hopane (Tm) in the m/z 191 chromatogram. ¹⁴Calculated from peak areas of C₂₉ 5 α (H), 14 α (H), 17 α (H)-24-ethyl-cholestane (20S + 20R) in the m/z 217 chromatogram. ¹⁵Calculated from peak areas of C₂₉ 5 α (H), 14 α (H), 17 α (H)-24-ethyl-cholestane (20S + 20R), and C₂₉ 5 α (H), 14 α (H), 17 α (H)-24-ethyl-cholestane (20S + 20R) in the m/z 217 chromatogram. ¹⁶Calculated from peak area of 25-*nor*-hopane (25-NH) in the chromatogram m/z 177 over peak area of C₃₀ 17 α (H), 21 β (H)-30-hopane (H30) in the m/z 191 chromatogram. ¹⁷Calculated from peak area of 25,28,30-tris-*nor*-hopane (25,28,30-TNH) in the m/z 177 chromatogram over peak area of C₃₀ 17 α (H), 21 β (H)-30-hopane (H30) in the m/z 191 chromatogram. ¹⁸Calculated from peak area of 25,30-bis-*nor*-hopane (25,30-BNH) in the m/z 177 chromatogram over peak area of C₃₀ 17 α (H), 21 β (H)-30-hopane (H30) in the m/z 191 chromatogram. ¹⁹Calculated from peak area of 25,28-bis-*nor*-hopane (25,28-BNH) in the m/z 177 chromatogram over peak area of C₃₀ 17 α (H), 21 β (H)-30-hopane (H30) in the m/z 191 chromatogram. ²⁰Calculated from peak area of C₃₀ 8,14-secohopane (SH30a) in the m/z 123 chromatogram over peak area of C₃₀ 17 α (H), 21 β (H)-30-hopane (H30) in the m/z 191 chromatogram.^{18,19,20} Proposed new geochemical parameters for heavy biodegradation.

GC×GC-TOFMS. The values observed for Oils #2 and #4 via GC×GC-TOFMS, however, indicate that the principal step of oil generation was reached. But, this parameter should be carefully analyzed because biodegraded oils could have a lower abundance of the R isomer, which is more susceptible to biodegradation. The homohopane H32 in the Oils #1 was not detected. This is suggested as being due to the severe biodegradation. The values observed for the H32S/(S+R) ratio showed no significant differences between the samples, and also between the two chromatographic techniques, GC-MS and GC×GC-TOFMS, with values between 0.51-0.54 and 0.54-0.57, respectively. This was also observed in a previous study in which the authors⁹ compared three techniques: GC-MS, GC-MRM-MS and GC×GC-TOFMS.

The Ts/(Ts + Tm) ratios are often used as a parameter of thermal maturity for the evaluation of oils from the same origin. The values observed for the Ts/(Ts + Tm) ratios showed no significant differences, varying from 0.37 to 0.4 via GC-MS and 0.36 and 0.41 by using GC×GC-TOFMS, with no distinction between both techniques. This can be explained by the fact that these two isomers, during a biodegradation process, are removed at the same rate, maintaining the initial ratio.⁶ Values around 1 for this ratio indicate that the oil has high thermal maturity.⁶ Thus, the values found for the Oils #2, #3 and #4 indicate that they have low thermal maturity or were possibly influenced by the biodegradation process.

The isomerization at C-20 in the C₂₉ 5 α (H),14 α (H),17 α (H)-steranes increases from zero to approximately 0.5, with the equilibrium value between 0.52 to 0.55 with the increasing maturity.^{6,32} The R configuration at C-20 occurs in steroid precursors existing in living organisms, and this is gradually converted during burial maturation to a mixture of the R and S sterane configurations.⁶ Data from Oil #2 using GC-MS and Oil #3 via GC×GC-TOFMS barely entered the oil generation range, while Oil #2, via GC×GC-TOFMS, reached the equilibrium value. Partial sterane biodegradation of oil can result in an increase of a α 20S/(20S + 20R) sterane ratios (C₂₇, C₂₈ and C₂₉) to above 0.55, which was observed in Oils #3 and #4 via GC-MS, and Oil #4 using GC×GC-TOFMS. This was due the selective removal of the a α 20R epimer by bacteria.³³ The greater stability of the 20S epimer compared to 20R is the main reason for increasing 20S/(20S + 20R) ratios with thermal maturity,³⁴ and there is no evidence for equilibration of 20S and 20R epimers. This ratio depends partly on the source rock and can decrease at high maturity.³⁵ Differential stability of epimers and generation of additional material from the kerogen may affect this ratio.³⁶ Other factors, such as organofacies

differences, weathering and biodegradation can affect the sterane isomerization ratios.⁶

The isomerization at the C-14 and C-17 positions in the 20S and 20R C₂₉ regular steranes causes an increase in the $\beta\beta/(\alpha\alpha + \beta\beta)$ from zero to approximately 0.7, with equilibrium value between 0.67 and 0.71, with the increasing maturity.^{6,32} This ratio appears to be independent of source organic matter input and is somewhat slower to reach equilibrium than the 20S/(20S + 20R) ratio, thus making it effective at higher levels of maturity. The increase in $\beta\beta/(\alpha\alpha + \beta\beta)$ ratio, as observed in Oil #3 via GC×GC-TOFMS (Table 2), indicates the loss by thermal degradation of the a α isomer. This is due to the fact that a α isomers are degraded more rapidly than ab β isomers.³⁷

Some studies^{6,37} indicate that changes in source and maturation parameters, traditionally associated with isomerization, are due to a combination of three processes: generation from kerogen, cracking and secondary isomerization.

Several factors, such as source of organic matter, lithology and depositional conditions, can influence biomarker maturation parameters.⁶ The factor of greatest importance for the variance is attributed to the biodegradation. However, it is difficult to determine the maturity parameters by using only hydrocarbon biomarker parameters that may have been altered by biodegradation.

Biodegradation

The biomarker composition of the oils in terms of relevant compound classes was estimated and assigned to the Peter & Moldowan (PM) scale, presented in Table 3. Based on these scales, the four oil samples can be classified as severely biodegraded (PM rank \geq 6), mainly because of the presence of the 25-nor-hopane and 25-nor-tricyclic terpane series in addition to that of nor-gammacerane.

The samples have distinct characteristics concerning to biodegradation, which can influence parameters related to thermal evolution and origin. Two distinct fingerprints, associated to degrees of alteration, were defined on the basis of biomarker composition (Figure 6). One of them is related to the presence of tetracyclic terpanes, steranes, hopanes (C₂₈-C₃₀), homohopanes (C₃₁-C₃₅), bis-nor-hopanes (BNH), 25,28,30-tris-nor-hopane (TNH), 25-nor-hopanes (C₂₆-C₃₄), nor-gammacerane, secohopanes and abundant n-alkanes. It includes the Oils #2, #3 and #4, with similar GC×GC-TOFMS profiles (Figures 6a and 6c). The detection of these compounds is characteristic of a mixture of biodegraded oils with a low abundance of non-biodegraded oils. On the other hand, the second fingerprint is characterized by the presence of the same

Table 3. Biomarker composition of the oils and Peter & Moldowan scale

Compound/Class	Oil # 1	Oil # 2	Oil # 3	Oil # 4	PM Scale	
<i>n</i> -Alkanes (GC-FID)	–	–	+	++	1	slight
Isoprenoids (GC-FID)	–	–	+	++	3	moderate
C ₂₉ 17 α (H),21 β (H)-25- <i>nor</i> -Hopane (GC-MS and GC \times GC-TOFMS)	++	++	++	++	4	heavy
25- <i>nor</i> -Hopanoid series (GC-MS and GC \times GC-TOFMS)	++	++	++	++	5	heavy
<i>nor</i> -Gammacerane (GC \times GC-TOFMS)	+	+	+	+	> 6	severe
25- <i>nor</i> -Tricyclic terpanes (GC-MS and GC \times GC-TOFMS)	+	++	++	++	> 6	severe
Hopanes destroyed (GC-MS)	+	–	–	–	> 6	severe
Steranes destroyed (GC-MS)	+	–	–	–	> 6	severe
25,30-Bis- <i>nor</i> -hopane (GC \times GC-TOFMS)	++	++	++	++		
25,28-Bis- <i>nor</i> -hopane (GC \times GC-TOFMS)	++	++	++	++		
25,28,30-Tris- <i>nor</i> -hopane (GC \times GC-TOFMS)	++	++	++	++		
PM Scale	> 6	> 6	> 6	> 6		
	severe	severe	severe	severe		

–: not detected; +: detected; ++: detected in higher abundance than +.

compounds except for *n*-alkanes, hopanes (C₂₈-C₂₉), homohopanes (C₃₁-C₃₅) and steranes, and includes only Oil #1. This sample is highly biodegraded, as evidenced by the predominant unresolved compound mixture (UCM), and absence of *n*-alkanes in the whole oil analysis (Figure S1 in the SI section). There is also a complete loss of *n*-alkanes, hopanes, homohopanes and steranes from the total ion chromatogram for Oil #1 (Figures 6b and 6d).

The absence of these compounds is characteristic of a severely biodegraded oil, and is consistent with residual material from the severe weathering and biodegradation of crude oil.³⁸

The tricyclic terpanes have advantages when used in correlations because they are less affected by maturation and biodegradation than hopanes and steranes.⁶ The tricyclic/hopane ratio increases with the elevation of thermal

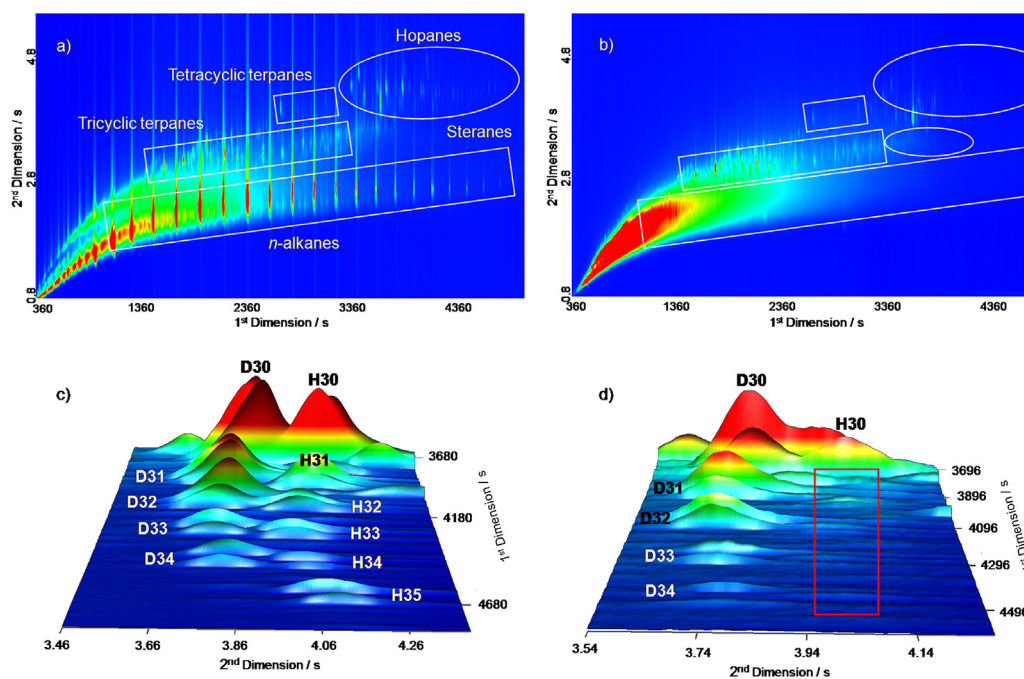


Figure 6. GC \times GC-TOFMS EIC *m/z* 191 and 177 of: (a) Oil #2, showing the presence of *n*-alkanes, tricyclic terpanes, tetracyclic terpanes, hopanes and steranes; (b) Oil #1, showing the absence the same compounds mentioned above; (c) Oil #2, showing the presence of homohopanes; (d) Oil #1, showing the absence of homohopanes.

maturity and biodegradation because the tricyclic terpanes are more resistant to biodegradation. In highly biodegraded oils when hopanes are removed, there is a rise in the relative abundance of the tricyclic compounds, increasing the values observed for the ratio tricyclic/hopane. The compound Tr23 is the most widely used on the tricyclic terpane ratio. The high values for the Tr23/H30 ratio (8, Table 2) in all samples are indicative of severe biodegradation.

The secohopanes are derived from the hopane or moretane series via the opening of the C-ring during the early stages of maturation and degradation of hydrocarbons⁶. These compounds are highly resistant to biodegradation.^{5,6} There are six possible configurations because of the stereochemistry of carbons 8 and 14, but all six secohopane configurations were not observed. This was most likely due to coelution combined with the low concentrations of these compounds in the oils. In this study, it was possible to identify secohopanes C₂₇ to C₃₃, with the highest concentrations observed in secohopanes C₂₉, C₃₀ and C₃₁ (mass spectra in Figure S4 in the SI section).³⁹

The detection of 25-*nor*-tricyclic terpanes, 25-*nor*-tetracyclic terpanes and 25-*nor*-hopanes was performed by monitoring the EIC *m/z* 177 (Figure 4). The complete series of 25-*nor*-hopanes (C₂₆-C₃₄ 25-*nor*-hopanes) was observed in all samples, including the C₂₄ demethylated tetracyclic terpane (DTe23) and the demethylated Ts, Tm and βTm. In addition, 25,30-BNH, 25,28-BNH and 25,28,30-TNH were also identified, with 25,30-BNH (mass spectrum in Figure S4 in the SI section) being the most intense at EIC *m/z* 177 (Figure 4). These compounds are indicative of severely biodegraded oil samples. This suggests that the hydrocarbons were exposed to severe conditions of biodegradation.^{6,25,40}

As already described, an important separation observed by GC×GC-TOFMS occurred between the isomers H30 and D30R.¹⁶ H30, the hopane found in most oils, decreases in concentration during biodegradation, while D30R is an intermediate of homohopane H31R degradation. If the H30 concentration decreases and the concentration of D30R increases due to oil biodegradation, this can mask the actual concentration of H30, which is widely used in the characterization of oils with respect to biodegradation using the 25-NH/H30 ratio, maturity and source parameters.⁶ The separation of these and other biomarkers is a favorable result of using GC×GC-TOFMS for oil characterization.

Many authors agree that 25-*nor*-hopanes indicate heavy biodegradation.^{5,6} The 25-*nor*-hopanes are a series of compounds, typical of many, but not all, heavily biodegraded oils. These compounds appear to result from the bacterial removal of the methyl group at C10 from the regular hopanes.⁵ Many biodegraded oils reported in the

literature contain abundant 25-*nor*-hopanes, evidence of severe biodegradation (rank ≥ 6).⁶

The 25-*nor*-hopane/hopane (25-NH/H30) ratio (16, Table 2) increases with the extent of biodegradation. Thus, it was possible to distinguish the degree of biodegradation of the samples based on the increasing 25-NH/H30 ratio, which had values between 1.36 and 6.04 as measured by GC×GC-TOFMS, and between 1.11 and 3.45 as measured by GC-MS (Table 2). As a result of the better chromatographic separation between 25,28,30-TNH from SH30, H30 and D30R from SH31 were achieved using GC×GC-TOFMS. Because of the detection of many abundant demethylated terpanes, three new parameters were proposed for the characterization of severe biodegradation: 25,28-BNH/H30 (18), 25,30-BNH/H30 (19) and SH30/H30 (20). These proposed biodegradation parameters showed a trend of biodegradation between the studied samples, indicating a decreasing order of biodegradation: Oil #1 > Oil #2 > Oil #3 > Oil #4. This demonstrates the same trend as the 25-NH/H30 ratio exhibited between the samples, which is the parameter usually employed for characterization of biodegraded oils.

The relation graphic between 25-NH/H30 with 25,30-BNH/H30, 25,28-BNH/H30 and SH30/H30 ratios, showed good correlation (R² greater than 0.9) between 25-NH/H30 with 25,30-BNH/H30, 25-NH/H30 with 25,28-BNH/H30, and 25-NH/H30 with SH30/H30 ratios, which can be observed across the correlation coefficient of 0.993, 0.9978 and 0.9201 respectively, as shown in Figure S3 in the SI section. According to the results obtained in this work, three new promising parameters may be proposed, but further investigation based on a larger number of severely biodegraded oils is required in order to verify and finally include them as biodegradation parameters. After the confirmation, the compounds 25,28-BNH, 25,30-BNH and SH30, and consequently the three new promising parameters on which they are based, 25,28-BNH/H30, 25,30-BNH/H30 and SH30/H30, should be routinely employed in future investigation, mainly for severely biodegraded oils. Thus, the potential of GC×GC-TOFMS to provide new biodegradation parameters is demonstrated in these results.

Origin and maturation ratios, as Hop/St, H30/C₂₇ ααα, Ts/Tm, Ts/(Ts + Tm), H32 S/(S + R), C₂₉ ααα S/(S + R) and C₂₉ ββ/(αα + ββ), did not vary significantly for these four samples using both GC-MS and GC×GC-TOFMS. However, for the biodegradation parameters as SH30a/H30 and 25,30-BNH/H30, this was not completely true. A significant change was observed, clearly showing the biodegradation effect, as presented in Table 2. Therefore, the SH30a/H30, 25,28,30-TNH and 25,30-BNH/H30 ratios

may also be applied routinely, beside the commonly used 25-NH/H30, 25,28,30-BNH/H30.

Conclusion

The oils from Colombia under investigation showed complete series of 25-*nor*-hopanes, some demethylated tricyclic terpanes, *nor*-gammacerane, C₂₉ 28-*nor*-spergulanes, 25,30-BNH, 25,28-BNH, 25,28,30-TNH and 8,14-secohopanes, which resulted from the heavy biodegradation that occurred in the reservoirs.

The higher chromatographic resolution and sensitivity of the GC×GC-TOFMS allowed for the separation and identification of individual compounds, which normally coelute in conventional GC-MS analyses. This contributes to a better characterization of the oil fractions. As result of the chromatographic separation between 25,28,30-TNH and SH30; H30, D30R, and SH31 by GC×GC-TOFMS, it was possible to propose three new parameters for heavy biodegradation: 25,28-BNH/H30, 25,30-BNH/H30 and SH30/H30. These proposed parameters showed a trend of biodegradation between the studied samples, indicating a decreasing order of biodegradation: Oil #1 > Oil #2 > Oil #3 > Oil #4. In addition, geochemical parameters such as origin, thermal maturity and environment deposition were calculated, demonstrating the applicability of GC×GC-TOFMS in biomarker ratios. So, the use of GC×GC-TOFMS in geochemical analyses can easily support oil exploration.

The samples showed a Hop/St ratio < 4, the predominance of C₂₇ steranes over C₂₉ homologous, the presence of C₃₀ steranes, low concentration of Tr19 and Tr20 when compared to Tr23, a condition which is indicative of marine oils. Moreover, the samples also showed H35/H34 ratio > 1 and the presence of 25,28,30-TNH signifying an anoxic depositional environment. The presence of Te24, gammacerane and Ts/Tm ratio < 1 suggests a carbonate or evaporitic depositional environment.

Supplementary Information

Supplementary information (Figure S1-S4 Table S1 in the SI section) is available free of charge at <http://jbcs.org.br> as a PDF file.

Acknowledgments

The authors thank Capes and CNPq (Brazilian research councils) for fellowships and financial support. Acknowledged is ICP-Ecopetrol for providing samples and Petrobras for their financial support.

References

1. Aitken, C. M.; Jones, D. M.; Larter, S. R.; *Nature* **2004**, *431*, 291.
2. Jones, D. M.; Head, I. M.; Gray, N. D.; Adams, J. J.; Rowa, A. K.; Aitken, C. M.; Bennett, B.; Huang, H.; Brown, A.; Bowler, B. F. J.; *Nature* **2007**, *451*, 176.
3. Wenger, L. M.; Davis, C. L.; Isaksen, G. H.; *SPE Reservoir Eval. Eng.* **2002**, *5*, 375.
4. Larter, S.; Huang, H.; Adams, J.; Bennett, B.; Snowdon, L. R.; *Org. Geochem.* **2012**, *45*, 66.
5. Peters, K. E.; Moldowan, J. M.; *The Biomarker Guide*, 1st ed.; Prentice Hall: New York, USA, 1993.
6. Peters, K. E.; Walters, C. C.; Moldowan, J. M.; *The Biomarker Guide: Biomarkers and Isotopes in Petroleum Exploration and Earth History*, vol. 2, 1st ed.; Cambridge University Press: Cambridge, UK, 2005.
7. Head, I. M.; Jones, D. M.; Larter, S. R.; *Nature* **2003**, *46*, 344.
8. Springer, M. V.; Garcia, D. F.; Gonçalves, F. T. T.; Landau, L.; Azevedo, D. A.; *Org. Geochem.* **2010**, *41*, 1013.
9. Eiserbeck, C.; Nelson, R. K.; Grice, K.; Curiale, J.; Reddy, C. M.; *Geochim. Cosmochim. Acta* **2012**, *87*, 299.
10. von Mühlen, C.; Zini, C. A.; Caramão, E. B.; *Quim. Nova* **2006**, *29*, 765.
11. Tran, T. C.; Logan, G. A.; Grosjean, E.; Ryan D.; Marriott, P. J.; *Geochim. Cosmochim. Acta* **2010**, *74*, 6468.
12. Moraes, M. S. A.; Zini, C. A.; Gomes, C. B.; Bortoluzzi, J. H.; von Mühlen, C.; Caramão, E. B.; *Quim. Nova* **2011**, *34*, 1188.
13. Silva, R. S. F.; Tamanqueira, J. B.; Dias, J. C. M.; Passarelli, F. M.; Bidart, A. M. F.; Aquino Neto, F. R.; Azevedo, D. A.; *J. Braz. Chem. Soc.* **2011**, *22*, 2121.
14. Ventura, G. T.; Kenig, F.; Reddy, C. M.; Frysinger, G. S.; Nelson, R. K.; Mooy, B. V.; Gaines, R. B.; *Org. Geochem.* **2008**, *39*, 846.
15. Aguiar, A.; Silva Jr., A. I.; Azevedo, D. A.; Aquino Neto, F. R.; *Fuel* **2010**, *89*, 2760.
16. Ávila, B. M. F.; Aguiar, A.; Gomes, A. O.; Azevedo, D. A.; *Org. Geochem.* **2010**, *41*, 863.
17. Ventura, G. T.; Simoneit, B. R. T.; Nelson, R. K.; Reddy, C. M.; *Org. Geochem.* **2012**, *45*, 48.
18. Silva, R. S. F.; Aguiar, H. G. M.; Rangel, M. D.; Azevedo, D. A.; Aquino Neto, F. R.; *Fuel* **2011**, *90*, 2694.
19. Ventura, G. T.; Raghuraman, B.; Nelson, R. K.; Mullins, O. C.; Reddy, C. M.; *Org. Geochem.* **2010**, *41*, 1026.
20. Grice, K.; Alexander, R.; Kagi, R. I.; *Org. Geochem.* **2000**, *31*, 67.
21. Azevedo, D. A.; Tamanqueira, J. B.; Dias, J. C. M.; Carmo, A. P. B.; Landau, L.; Gonçalves, F. T. T.; *Fuel* **2008**, *87*, 2122.
22. Silva, T. F.; Azevedo, D. A.; Rangel, M. D.; Fontes, R. A.; Aquino Neto, F. R.; *Org. Geochem.* **2008**, *39*, 1249.

23. Oliveira, C. R.; Ferreira, A. A.; Oliveira, C. J. F.; Azevedo, D. A.; Santos Neto, E. V.; Aquino Neto, F. R.; *Org. Geochem.* **2012**, *46*, 154.
24. Frysinger, G. S.; Gaines, R. B.; *J. Sep. Sci.* **2001**, *24*, 87.
25. Nytoft, H. P.; Bojesen-Koefoed, J. A.; Christiansen, F. G.; *Org. Geochem.* **2000**, *31*, 25.
26. Nytoft, H. P.; Bojesen-Koefoed, J. A.; Christiansen, F. G.; Fowler, M. G.; *Org. Geochem.* **2002**, *33*, 1225.
27. Nytoft, H. P.; Lutnaes, B. F.; Johansen, J. E.; *Org. Geochem.* **2006**, *37*, 772.
28. Wang, Z.; Stout, S. A.; Fingas, M.; *Environ. Forensics* **2006**, *7*, 105.
29. Hegazi, A. H.; El-Gayar, M. Sh.; *J. Pet. Geol.* **2009**, *32*, 343.
30. Clark, J. P.; Philp, R. P.; *Bull. Can. Petrol. Geol.* **1989**, *37*, 401.
31. Seifert, W. K.; Moldowan, J. M.; *Phys. Chem. Earth* **1980**, *12*, 229.
32. Seifert, W. K.; Moldowan, J. M. In *Methods in Geochemistry and Geophysics*; Johns, R. B., ed.; Elsevier: Amsterdam, The Netherlands, 1986, ch. 24, p. 261.
33. Seifert, W. K.; Moldowan, J. M.; Demaison, G. J.; *Org. Geochem.* **1984**, *6*, 633.
34. Requejo, A. G.; Allan, J.; Creaney, S.; Gray, N. R.; Cole, K. S.; *Org. Geochem.* **1992**, *22*, 441.
35. Peter, K. E.; Moldovan, J. M.; Sundararaman, P.; *Org. Geochem.* **1990**, *15*, 249.
36. Dzou, L. I.; Noble, R. A.; Senftle, J. T.; *Org. Geochem.* **1995**, *23*, 681.
37. Farrimond, P.; Taylor, T.; Telnaes, N.; *Org. Geochem.* **1998**, *29*, 1181.
38. Fazeelat, T.; Alexander, R.; Kagi, R. I.; *Org. Geochem.* **1994**, *21*, 257.
39. Wang, T. G.; Simoneit, B. R. T.; Philp, R. P.; Yu, C. P.; *Energy Fuels* **1999**, *4*, 177.
40. Fazeelat, T.; Alexander, R.; Kagi, R. I.; *Org. Geochem.* **1995**, *23*, 641.

Submitted: January 22, 2013

Published online: August 23, 2013

Supplementary Information

Comprehensive Two-Dimensional Gas Chromatography Coupled to Time of Flight Mass Spectrometry: New Biomarker Parameter Proposition for the Characterization of Biodegraded Oil

Renata F. Soares,*^a Ricardo Pereira,^a Raphael S. F. Silva,^a Leonardo Mogollon^b and Débora A. Azevedo*^a

^aInstituto de Química, Universidade Federal do Rio de Janeiro, Ilha do Fundão, 21941-909 Rio de Janeiro-RJ, Brazil

^bInstituto Colombiano del Petróleo, ECOPETROL S. A., Bucaramanga, Colombia

Table S1. Table of abbreviations

Trn	C _n tricyclic terpane	D33	17α(H),21β(H)-25-nor-30,31,32,33-tetrakishomohopane (22S + 22R)
Ten	C _n tetracyclic terpane	D34	17α(H),21β(H)-25-nor-30,31,32,33,34-pentakishomohopane (22S + 22R)
Ts	18α(H),21β(H)-22,29,30-tris-nor-neohopane	M29	17B(H),21A(H)-30-nor-hopane
Tm	17α(H),21β(H)-22,29,30-tris-nor-hopane	M30	C ₃₀ 17B(H),21A(H)-hopane
DTs	demethylated Ts; 18α(H),21β(H)-22,25,29,30-tetra-nor-neohopane	NH30	17α(H),30-nor-29-homohopane
DTm	demethylated Tm; 17α(H), 21β(H)-22,25,29,30-tetra-nor-hopane	29NSP	C ₂₉ 28-nor-spergulane
H28	17a(H),18a(H),21b(H)-28,30-bis-nor-hopane	NG	nor-gammacerane
H29	17A(H),21B(H)-30-nor-hopane	25-NH	C ₂₉ 17α(H),21β(H)-25-nor-hopane
C29Ts	18α(H),21β(H)-30-nor-neohopane	TPP	tetracyclic polyprenoid
H30	C ₃₀ 17a(H),21b(H)-30-hopane	Gam	gammacerane
H31	17α(H),21β(H)-30-homohopane (22S + 22R)	OL	oleanane
H32	17α(H),21β(H)-30,31-bishomohopane (22S + 22R)	25,28-BNH	17α(H),18α(H),21β(H)-25,28-bis-nor-hopane
H33	17α(H),21β(H)-30,31,32-trishomohopane (22S + 22R)	25,30-BNH	17α(H),18α(H),21β(H)- 25,30-bis-nor-hopane
H34	17α(H),21β(H)-30,31,32,33-tetrakishomohopane (22S + 22R)	25,28,30-TNH	17α(H),18α(H),21β(H)-25,28,30-tris-nor-hopane
H35	17α(H),21β(H)-30,31,32,33,34-pentakishomohopane (22S + 22R)	SH	secohopane
D30	17α(H),21β(H)-25-nor-30-homohopane (22S + 22R)	St	sterane
D31	17α(H),21β(H)-25-nor-30,31-bishomohopane (22S + 22R)	C _n ααα(Σ+P)	C _n sterane ααα (C ₂₇ -C ₃₀) (S + R)
D32	17α(H),21β(H)-25-nor-30,31,32-trishomohopane (22S + 22R)	C _n αββ(Σ+P)	C _n sterane αββ (C ₂₇ -C ₃₀) (S + R)
		Dia 27	C ₂₇ diasterane

*e-mail: renata_filgueiras@yahoo.com.br, debora@iq.ufrj.br

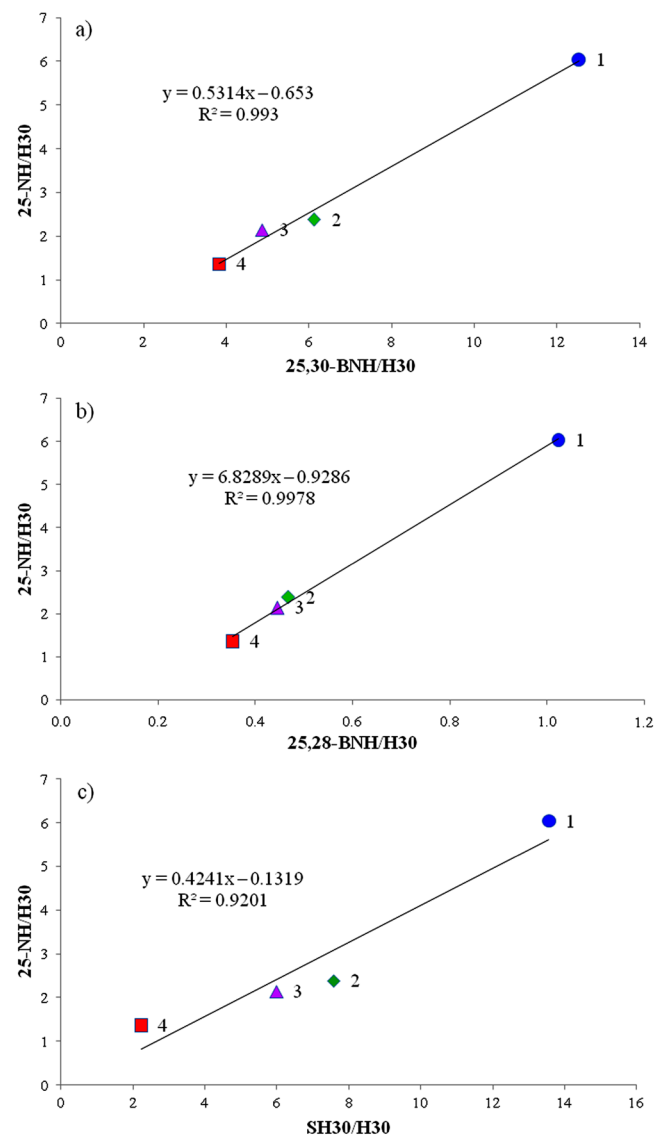


Figure S2. Correlation graphics between: (a) 25,30-BNH/H30 and 25-NH/H30, (b) 25,28-BNH/H30 and 25-NH/H30, (c) SH30/H30 and 25-NH/H30.

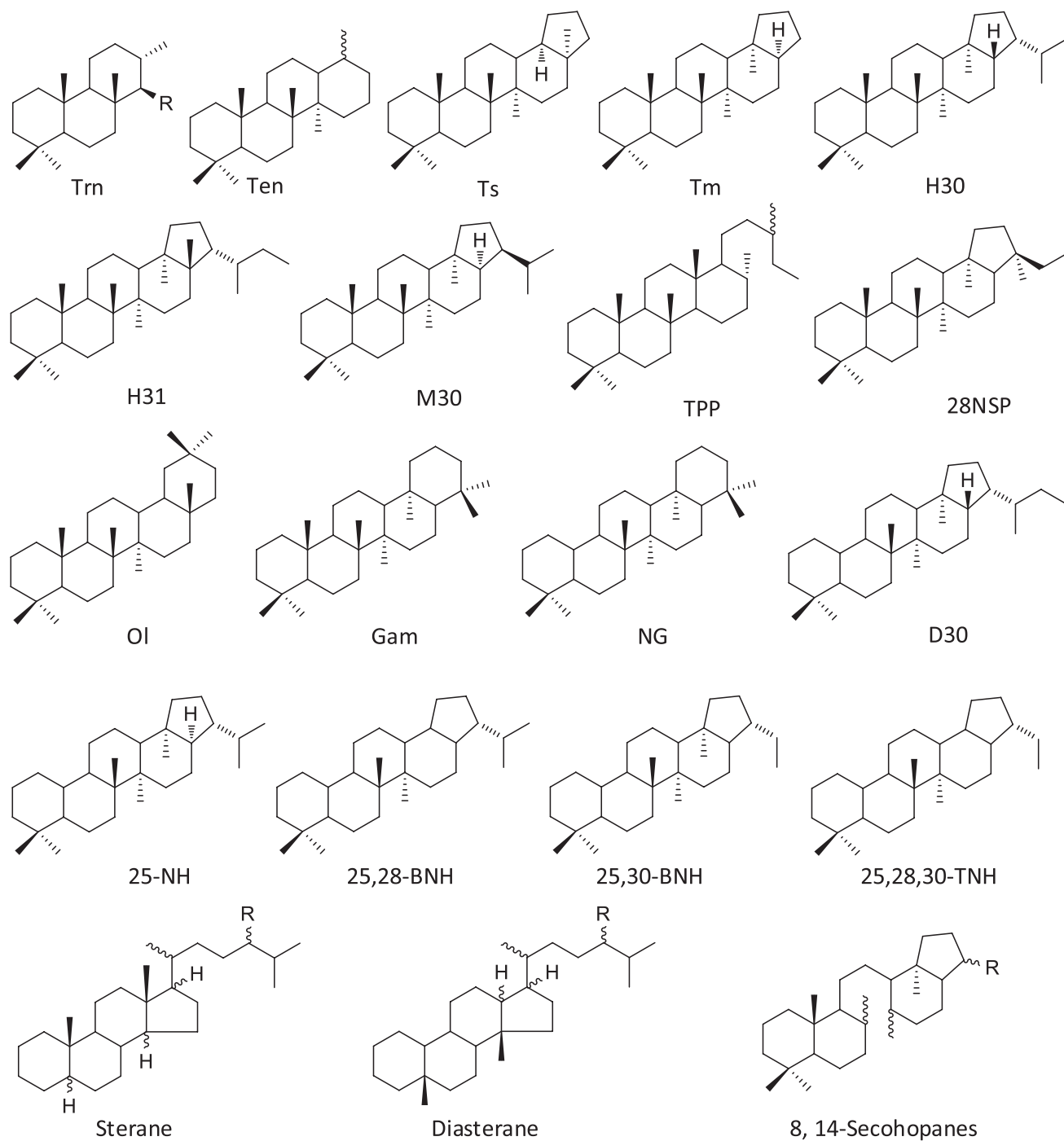


Figure S3. Selected structures of cited compounds.

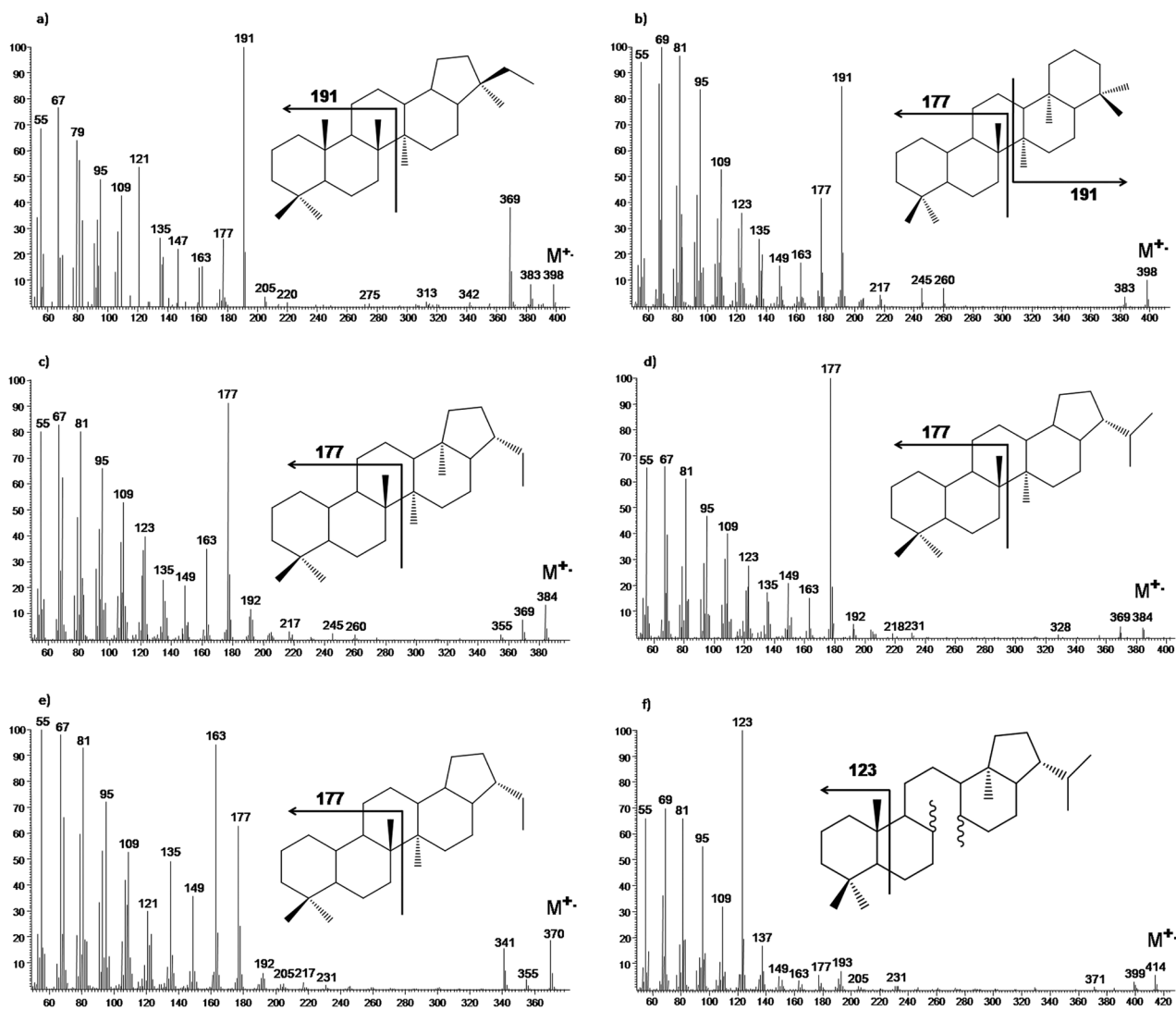


Figure S4. Mass spectra of: (a) C_{29} 28-nor-spergulane, (b) nor-gammacerane, (c) 25,30-bis-nor-hopane (25,30-BNH), (d) 25,28-bis-nor-hopane (25,28-BNH), (e) 25,28,30-tris-nor-hopane (25,28,30-TNH) and (f) C_{30} 8,14-secohopane with the fragmentation which leads to the diagnostic ion.